Article published online: 2023-10-16

Ultrasound Imaging of Thyroid Pathologies: A Pictorial Review

Supraja Laguduva Mohan[1] Ramkumar Govindarajalou[1] Sunitha Vellathussery Chakkalakkoombil[1] Madhan Ramachandran[1] Karthik Venkatesh[1]

[1] Department of Radiodiagnosis, Jawaharlal Institute of Postgraduate Medical Education and Research, Puducherry, India

Indographics 2023;2:79–94.

Address for correspondence Dr. Ramkumar Govindarajalou, MD, Department of Radiodiagnosis, Jawaharlal Institute of Postgraduate Medical Education and Research, Puducherry 605006, India (e-mail: gramk80@gmail.com).

Abstract

With its complex embryological origin, the thyroid can be affected by various congenital, developmental, benign, and malignant pathologies. Ultrasound, which is free from radiation and offers good spatial resolution, is the initial modality of choice in congenital hypothyroidism and is used in conjunction with scintigraphy. High-resolution ultrasound also aids in early diagnosis, risk stratification, and follow-up of nodules. While fine-needle aspiration cytology is the preferred method for further evaluation of thyroid nodules, ultrasound guidance reduces the likelihood of obtaining nondiagnostic samples. Numerous risk stratification guidelines for thyroid nodules have been developed by various societies over the past decade, with the most popular being the American College of Radiology—Thyroid Imaging Reporting and Data System. A comprehensive understanding of the varying morphological appearances of thyroid nodules and the consistent use of risk stratification guidelines can accurately detect incidental malignancies while avoiding unnecessary intervention in seemingly benign nodules.

Keywords

- thyroid nodules
- TI-RADS
- colloid nodules
- papillary carcinoma
- thyroglossal duct
- thyroid dysgenesis
- thyroiditis

Introduction

Thyroid disease is one of the most common endocrine diseases, with an estimated prevalence of approximately 42 million people suffering from thyroid disease in India.[1] The disease processes can be congenital, developmental, inflammatory, or neoplastic, affecting both children and adults. Thyroid nodules are common in women and the elderly and are attributed to hormonal, environmental, genetic, and hereditary factors.[2] The incidence of thyroid nodules ranges from 20 to 76%, with increasing diagnosis of incidental nodules on high-resolution ultrasonography.[2] Fine-needle aspiration cytology (FNAC) is a cost-effective and minimally invasive test of choice in establishing a definitive diagnosis of these nodules. Malignant disease is, however, seen in only 5 to 10% of thyroid nodules.[3] Hence, various imaging based TIRADS (Thyroid Imaging Reporting and Data System) guidelines have been devised for risk stratification of the nodules and reduction of unnecessary FNACs. This pictorial review gives an overview of ultrasound imaging techniques, imaging anatomy, developmental, benign, and malignant thyroid pathologies, and imaging guidelines for reporting of thyroid nodules.

Embryology and Anatomy of Thyroid Gland

The thyroid is a shield-shaped organ in the anterior aspect of the neck ("Thyreos" means shield in Greek).[4] During the 4th week of intrauterine life, a small diverticulum develops from

DOI https://doi.org/10.1055/s-0043-1772768.
ISSN 2583-8229.

© 2023. Indographics. All rights reserved.
This is an open access article published by Thieme under the terms of the Creative Commons Attribution-NonDerivative-NonCommercial-License, permitting copying and reproduction so long as the original work is given appropriate credit. Contents may not be used for commercial purposes, or adapted, remixed, transformed or built upon. (https://creativecommons.org/licenses/by-nc-nd/4.0/)

Thieme Medical and Scientific Publishers Pvt. Ltd., A-12, 2nd Floor, Sector 2, Noida-201301 UP, India

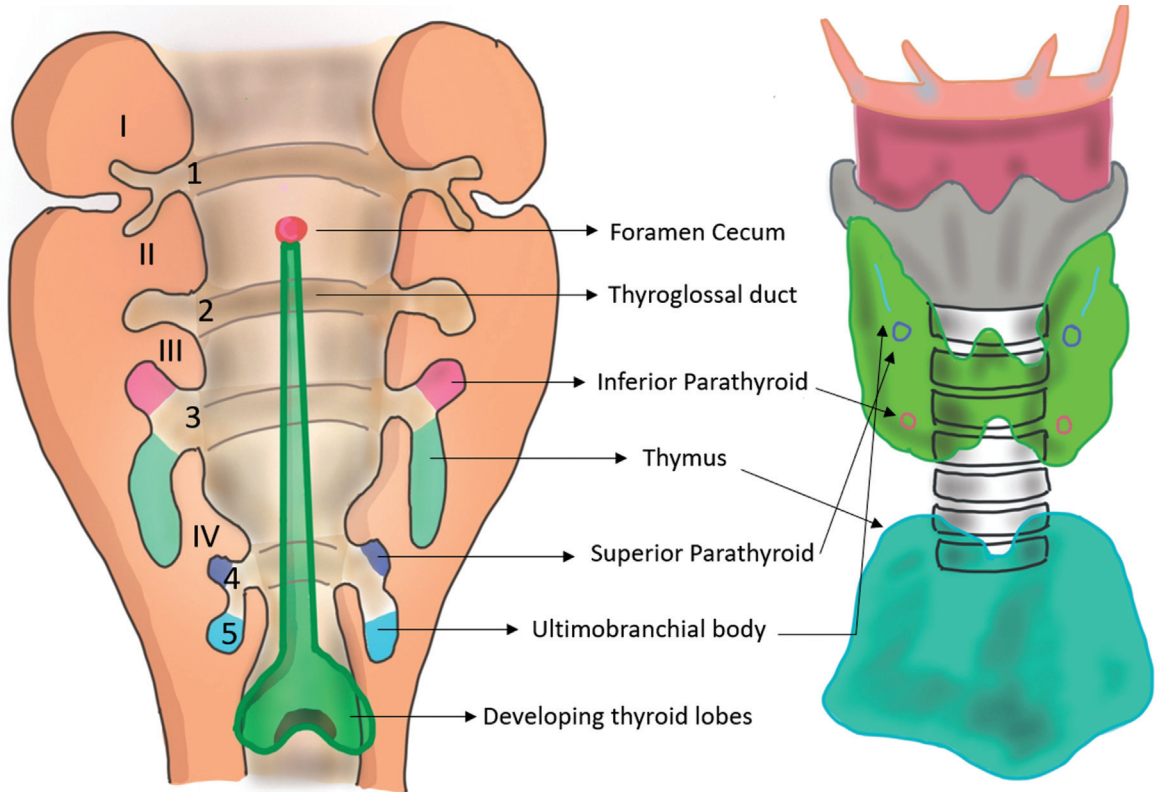

Fig. 1 Schematic diagram of development of the thyroid gland. Embryological location on the left, and final location after complete development on the right. The primitive thyroid gland (green) with the thyroglossal duct migrate from the foramen cecum into the neck. The pharyngeal pouches form the ultimobranchial body (4th and 5th) that forms the C–cells, superior (4th), inferior parathyroid glands (3rd), and the thymus (3rd and 4th).

the ventral wall of the primitive pharynx in the midline. This primitive gland grows and migrates to the lower part of the neck coursing anterior to the hyoid and larynx. The tract between the pharynx and the migrated thyroid, called the thyroglossal duct, normally involutes at a later stage and only a small pit called foramen cecum remains in the dorsum of the tongue (►**Fig. 1**). The primitive gland gives rise to the follicular cells, which secrete thyroid hormones. Parafollicular C cells, which secrete calcitonin, arise from the neural crest cells, which migrate into fourth and fifth pharyngeal pouches forming the ultimobranchial body. Migration completes by the 7th week of intrauterine life, and the production of thyroid hormone starts from the 12th week of gestation itself.[4,5] The fully developed thyroid gland comprises two lobes, connected by the isthmus at the level of second and third tracheal rings. It is located in the visceral space of the neck, related to the trachea and prevertebral space posteriorly, and to the sternohyoid and sternothyroid muscles anteriorly.

Ultrasound Imaging Techniques in the Evaluation of Thyroid

Being a superficial structure, ultrasound is considered the imaging modality of choice in the evaluation of thyroid pathologies, characterization of nodules, and calculation of thyroid volume.[6] High-resolution (7.5–13 MHz) linear array transducers are generally preferred, while lower frequency transducers can be used for larger nodules and masses. The patient lies in the supine position, with a pillow under the shoulder to facilitate hyperextension of the neck. The thyroid is evaluated for nodules, echogenicity, and vascularity. The normal thyroid gland is well-defined, shows uniform homogeneous echotexture, is more hyperechoic than adjacent muscle, with each lobe measuring approximately 4 to 6 cm craniocaudally (CC) and 1.3 to 1.8 cm in the anteroposterior (AP) and transverse (T) dimensions.[4,7] The volume of each lobe is calculated using the ellipsoid formula ($AP \times T \times CC \times 0.52$) and ranges from 10 to 20 mL in adults.[6] Color Doppler imaging, at a low flow setting, is used to assess the vascularity of the gland as well as nodules. Elastography is a frequently used adjunct technique which measures the hardness of tissues and, thereby, can help to differentiate benign and malignant nodules. There are two types of elastography techniques used in routine practice for thyroid nodules: (1) strain elastography, which depends on the deformation of tissues in response to mechanical stress (manual compression by the probe or using carotid artery pulsations as an internal compression source or by focused ultrasound waves in acoustic radiation force impulse (ARFI) imaging) and (2) shear wave elastography (SWE), which tracks the attenuation of acoustic pulses called shear waves traveling perpendicular to the direction of the ultrasound beam.[8] Contrast-enhanced ultrasound (CEUS) is also an additional technique that demonstrates the tumor microvascularization by intravenous injection of microbubbles (Sulfur Hexafluoride,

 © 2023. Indographics. All rights reserved.

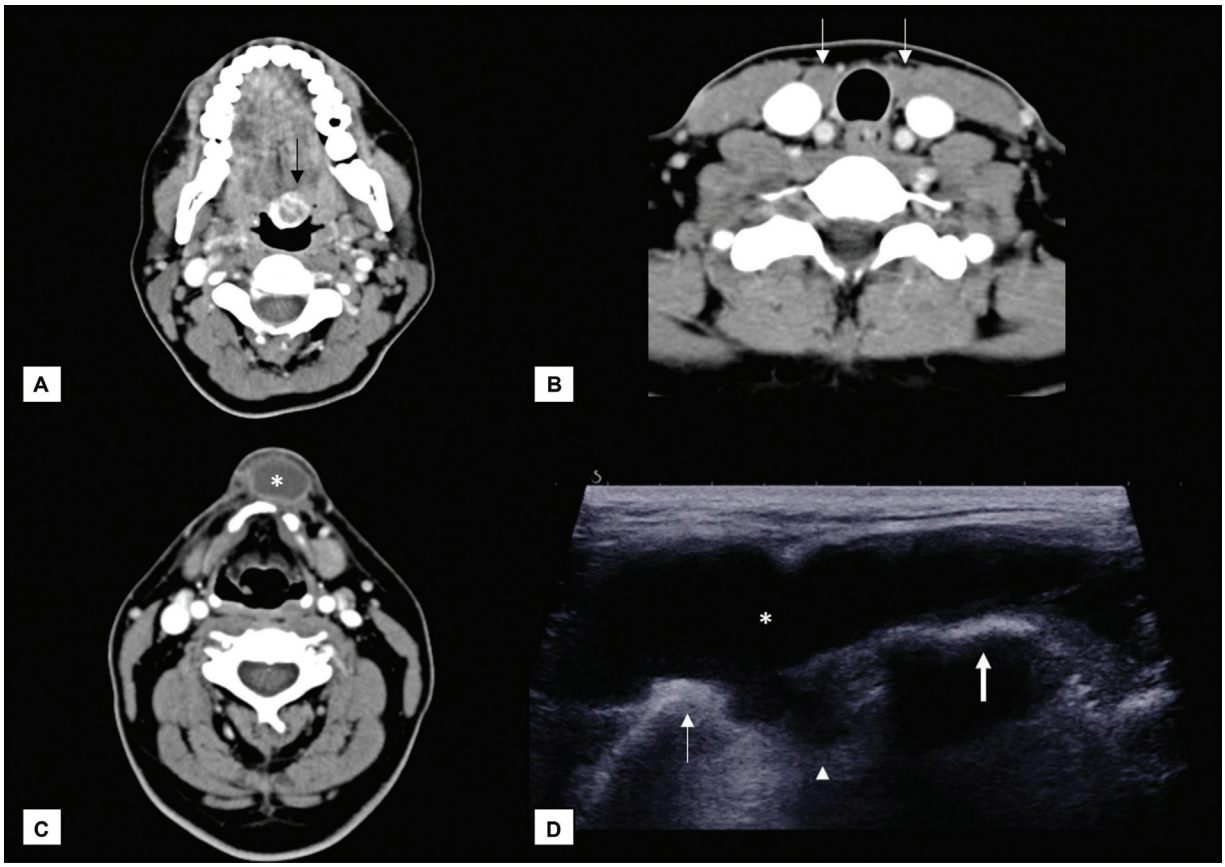

Fig. 2 Ectopic lingual thyroid (**A** and **B**). Axial contrast-enhanced CT images showing an intensely enhancing lesion at the base of tongue (*black arrow* in **A**) and absence of normal thyroid (*white arrows* in **b**). Thyroglossal cyst (**C** and **D**). Axial contrast-enhanced CT image shows a thick-walled cystic lesion (*asterisk* in **c**) in the midline of neck just anterior to the thyroid cartilage. Longitudinal ultrasound view (**D**) shows a cystic lesion (*asterisk*) anterior to the hyoid (*white arrow*) and thyroid (*thick white arrow*) cartilages, with part of the lesion extending between them (*arrow head*).

SonoVue, 1.2–4.8 mL followed by saline flush). The degree of enhancement (more, less, or equal to normal thyroid), pattern (centripetal or centrifugal or scattered), homogeneity, wash-in and wash-out times, and other features like ring enhancement help in the differentiation of benign and malignant nodules.[9]

Thyroid Pathologies

Congenital and Developmental

Thyroid Dysgenesis

Dysgenesis of the thyroid includes "ectopia" due to abnormal migration of the gland, "agenesis or athyreosis" where the gland is absent, and "hypoplasia" when it is not optimally developed. Normal thyroid volume (both lobes) ranges from 0.3 to 4 mL in neonates and infants to 1.7 to 6.4 mL by 6 to 8 years and 3 to 8.7 mL by 9 to 11 years of age and is slightly more in girls.[10] Ectopic thyroid tissue can be found anywhere along the course of the thyroglossal duct, most commonly (90%) at the base of the tongue (►**Fig. 2**). Thyroid scintigraphy is the gold standard for the evaluation of children with congenital hypothyroidism. The thyroid may appear normal on ultrasound in hypoplasia, but scintigraphy can still show poor uptake.[11] Occasionally, one or more cysts can also be found in the region of the hypoplastic or absent thyroid (►**Fig. 3**). They are hypothesized to be remnants of the ultimobranchial body or the thyroglossal duct.[12]

Lack of Obliteration of Thyroglossal Duct

Patency of the thyroglossal duct can lead to the formation of cyst, sinus, or fistula. Thyroglossal duct cyst is the most common congenital neck mass (►**Fig. 2**). The thyroglossal duct loops in between the developing hyoid bone and thyroid cartilage. This creates a tail of the cyst coursing beneath the hyoid, a feature that helps to differentiate it from other neck cysts. Thyroglossal ducts cysts are seen in the midline, occasionally paramedian, and can be suprahyoid, at the level of hyoid or commonly infrahyoid.[13] Thyroglossal fistulas (►**Fig. 4**) can open at the foramen cecum above till the lower part of the neck below with numerous side branches. The persistent tract may also form ramifications within the hyoid bone or its periosteum.[14]

Benign

Simple or Hemorrhagic Cyst

Cysts are thought to occur due to an ischemic episode that creates necrosis. This can happen congenitally, developmentally, or due to tumors, most commonly in papillary thyroid

 © 2023. Indographics. All rights reserved.

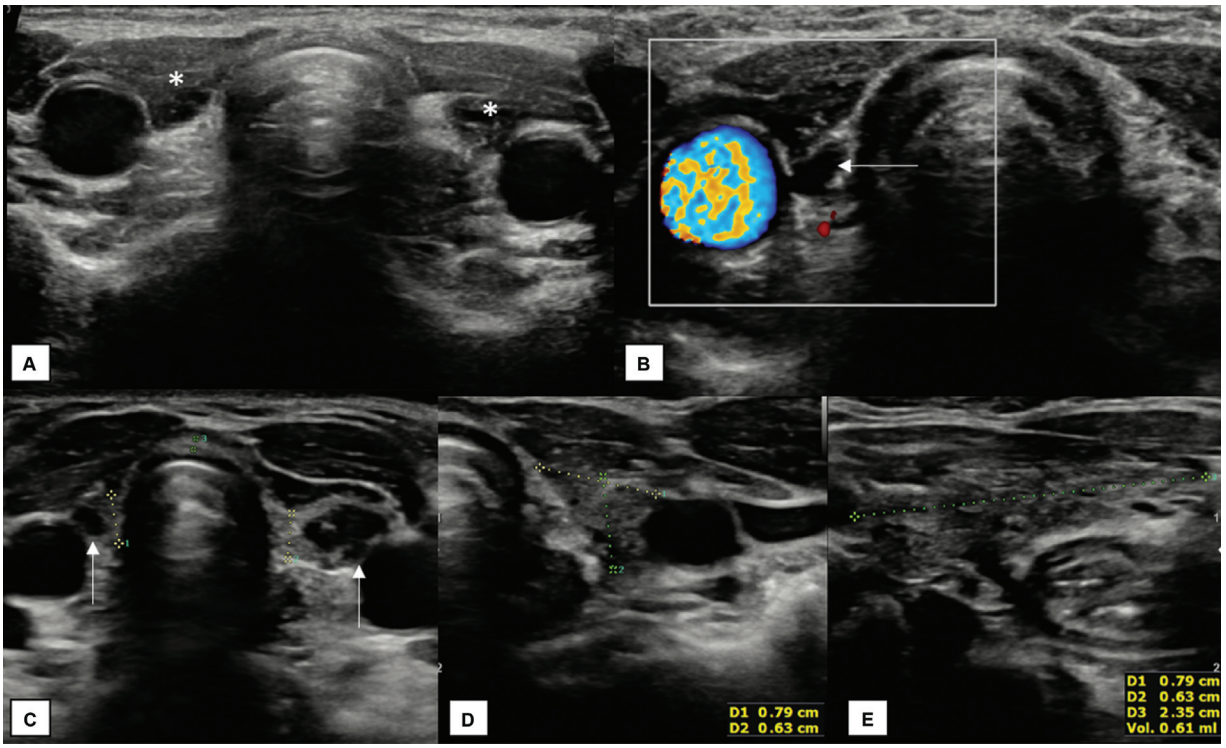

Fig. 3 Thyroid dysgenesis. Transverse views of an infant's thyroid (**A** and **B**) showing the absence of thyroid tissue with strap muscles filling the thyroid region (*asterisks*). Cystic remnants are seen in the right paratracheal region (*arrow* in **B**). Similar cystic changes within hypoplastic thyroid tissue are seen in (**C**) (*arrows*). Objective evaluation of hypoplasia by measurement of thyroid volume in hypoplasia in a 6-year-old child (**D** and **E**) showing a volume of 0.61 mL, much less than the reference range (1.7–6.4 mL).

carcinoma. A simple cyst without any septation or solid component is considered to be benign (►**Fig. 5**).[15]

Benign Follicular Nodule

It includes colloid nodules, nodular goiter, hyperplastic nodules, nodules in Grave's disease, and macrofollicular subtype of follicular adenoma. All such nodules have a varying composition of follicular cells and colloid within—with more colloid in colloid nodules and more follicular cells and varying fibrosis in hyperplastic nodules (►**Figs. 5** and **6**). Calcification of inspissated colloid is responsible for the comet tail artifacts, seen on ultrasound.[15]

Thyroiditis

Diffuse inflammation of the thyroid (thyroiditis) can be classified into acute infectious, autoimmune (Grave's and Hashimoto), subacute granulomatous (De Quervain's) thyroiditis, and fibrous (Riedel's) thyroiditis. The thyroid becomes diffusely heterogeneous and hypoechoic (due to lymphocytes) with increased vascularity and micronodules, particularly in Hashimoto thyroiditis (►**Fig. 7**). There is also an increased risk of primary thyroid lymphoma and papillary carcinoma in Hashimoto thyroiditis.[16] Occasionally, thyroiditis can itself be focal, accounting to approximately 5.3% of all thyroid nodules.[17] Differentiation between different types of thyroiditis or nodular thyroiditis from other follicular nodules on ultrasound is not possible due to overlapping and variable imaging appearance.[16,18]

Follicular Adenoma

It is a benign encapsulated neoplasm made up of follicular cells. Follicular adenomas and carcinomas cannot usually be differentiated on ultrasound or FNAC; a biopsy is needed to assess the vascular invasion in carcinomas. However, recent studies suggest that the presence of nodules within nodule appearance along with calcifications is more likely in follicular carcinomas.[19]

Malignant

Papillary Carcinoma

It is the most common thyroid malignancy (80%) and includes cells arranged in the form of papillae or monolayers. Psammoma bodies and cystic changes are typically associated with them, which correspond to microcalcifications and anechoic areas on ultrasound in the nodule and their nodal metastases (►**Fig. 8**).[7] The follicular variant appears larger and shows more benign sonographic features.[20] It has a very favorable prognosis when treated early, especially in patients who are below 30 years of age.[15]

Follicular Carcinoma

It constitutes 11% of thyroid malignancies. Here, the neoplastic follicular cells show capsular or vascular invasion and have a propensity for hematogenous spread, most commonly to bone and lungs (►**Fig. 9**). Hurthle cell carcinoma is a variant of follicular carcinoma with oncocytic cells, which has an aggressive course and poor prognosis.[7]

 © 2023. Indographics. All rights reserved.

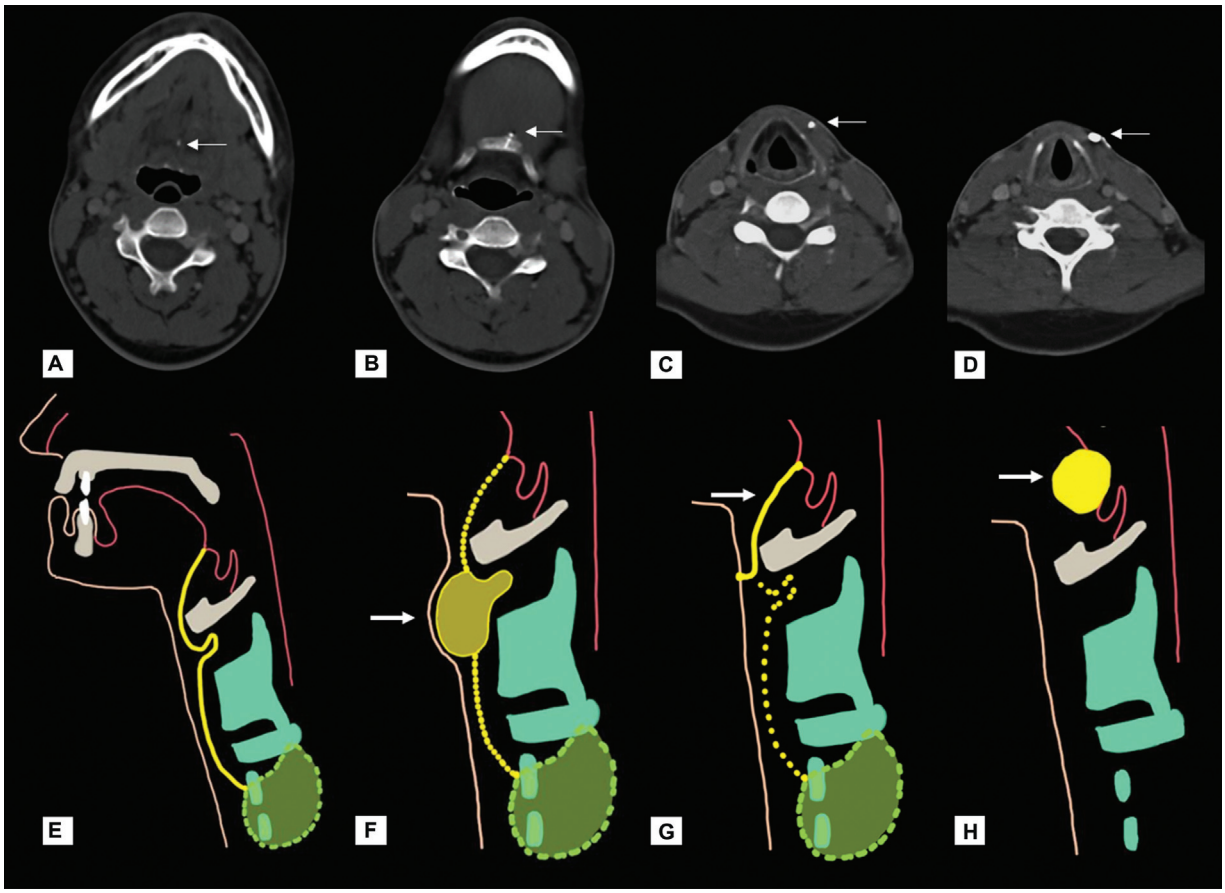

Fig. 4 Thyroglossal fistula (**A–D**). Axial unenhanced CT images with injection of contrast into an opening in the left lateral aspect of neck (**D**) show a fistulous tract (white arrows) opening into the region of foramen cecum (**A**). Schematic diagram of thyroglossal duct and related anomalies (**E–H**). (**E**) The normal course of the thyroglossal duct (*yellow*) from foramen cecum to the thyroid, with an inward looping between the hyoid and thyroid cartilages. The lack of obliteration at various levels give rise to thyroglossal cyst (**F**), fistula (**G**), and ectopic thyroid (**H**).

Medullary Carcinoma

It constitutes 4% of thyroid malignancies with an intermediate prognosis.[7] Arising from the C cells, this tumor produces calcitonin, and it cannot take up iodine. It is most commonly (80%) sporadic. Twenty percent can be familial—either related to MEN 2a, MEN 2b, or non-MEN. Compared with papillary carcinomas, they are larger, more heterogeneous, and vascular on ultrasound (►**Fig. 10**).[21]

Anaplastic Carcinoma

It is a rare thyroid malignancy with aggressive local invasion, amounting to only up to 2% of the total (►**Fig. 10**). The malignant cells are undifferentiated; hence cannot take up iodine and are unsuitable for radioablation.[7] Most of the patients have a history of long-standing goiter, as the tumor arises from the transformation of well-defined carcinoma or adenoma. It shows rapid growth and compressive symptoms.[15]

Lymphoma

Primary lymphoma is rare (1 to 5% of thyroid malignancies). Hashimoto thyroiditis is a predisposing factor. It can be nodular, diffuse, or mixed (►**Fig. 10**). The nondiffuse types are markedly hypoechoic and have been referred to as pseudocysts. Lesions can be multifocal, hypervascular, and calcification is uncommon.[22]

Metastasis

It is rare and occurs in patients who already have widespread metastasis in other organs. The most commonly reported tumors metastasizing to the thyroid include lung, breast, renal malignancies, and melanoma.[23]

Evaluation of Nodules and Risk Stratification

Since 2009, various risk stratification algorithms (TIRADS) have come up for thyroid nodules, of which the most commonly used one is that of the American College of Radiology (ACR).[24,25] Point scores are given for each morphological feature (►**Fig. 11**) and the final score and size are used to decide the need for FNAC or follow-up (►**Table 1**).

Evaluation of Thyroid Nodules on Ultrasonography

Composition: Nodules can be solid, mixed solid cystic, entirely cystic, or spongiform. Among these, solid nodules have the highest risk of malignancy.[26] Spongiform nodules, characterized by multiple microcystic areas forming more

 © 2023. Indographics. All rights reserved.

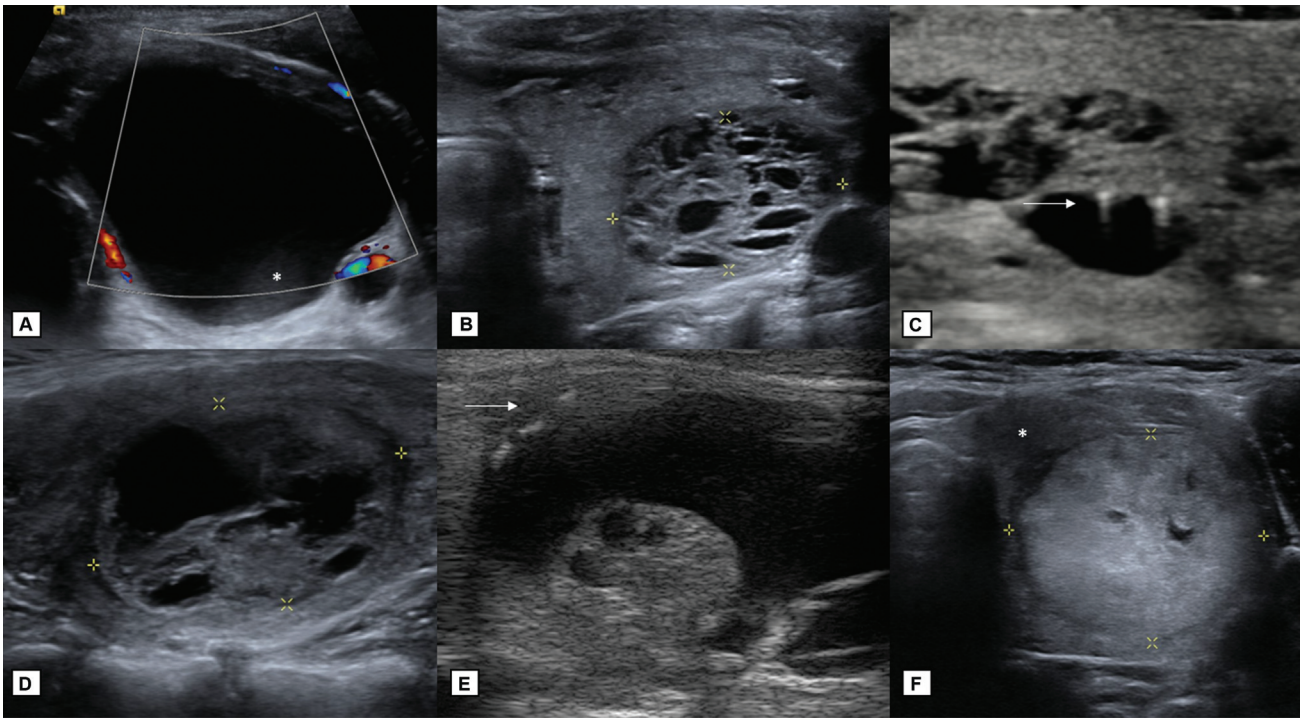

Fig. 5 Benign thyroid nodules. TR1—Completely cystic nodule with dependent colloid (*asterisk* in **A**), TR 1—spongiform nodule with more than 50% cystic spaces (**B**), comet tail artifact (arrow in **C**), TR 2—solid cystic isoechoic nodule (**D**), TR3—solid cystic isoechoic nodule with macrocalcification (*arrow* in **E**), and TR 3—solid nodule more echogenic than the adjacent parenchyma (*asterisk* in **F**). All the nodules were colloid or nodular goiters by FNAC (Bethesda II).

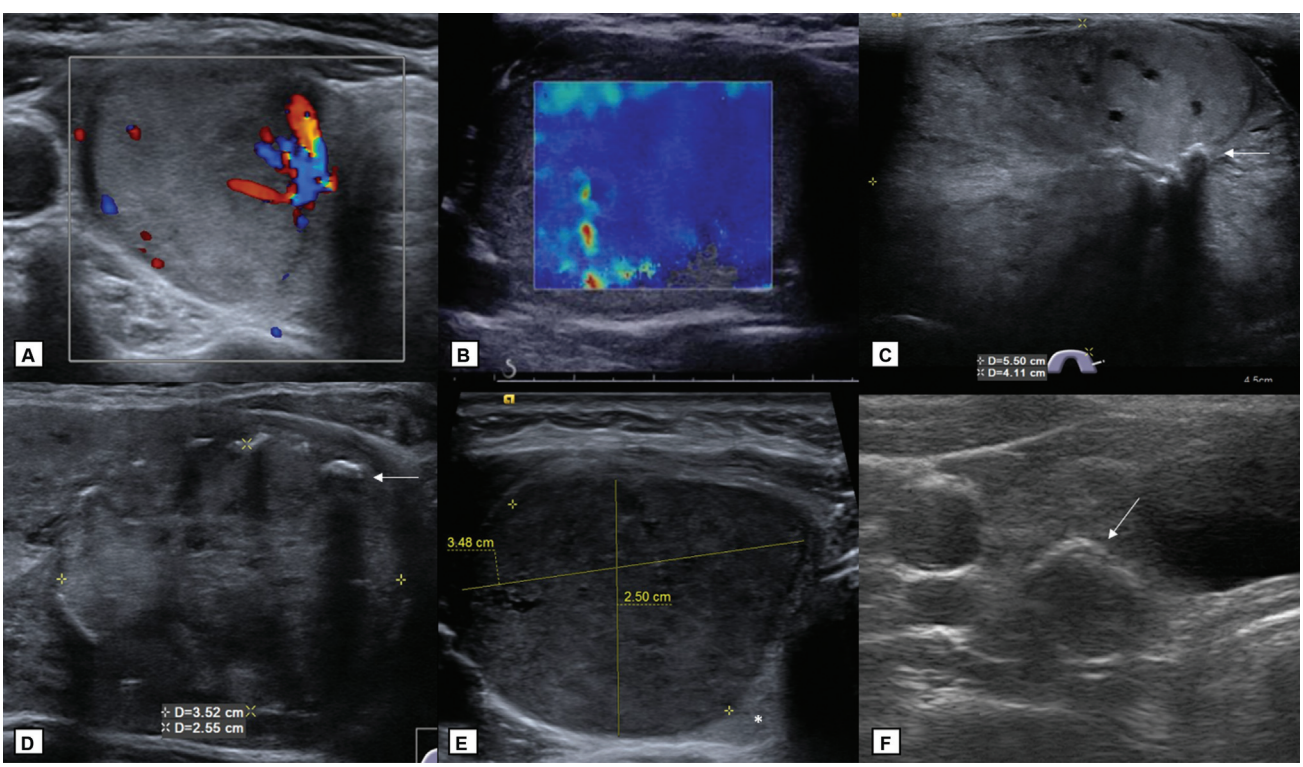

Fig. 6 Benign thyroid nodules. TR3—Solid isoechoic nodule with peripheral vascularity (**A**), soft on elastography (**B**), TR 4—Solid isoechoic nodule with macrocalcifications (*arrow* in **C**), TR 4—Solid isoechoic with interrupted rim calcification (*arrow* in **D**), TR 4—Solid nodule hypoechoic compared with the adjacent parenchyma (*asterisk* in **E**), and TR 4—Solid hypoechoic nodule with rim calcification (*arrow* in **F**). FNAC proved them to be nodular goiters (Bethesda II).

 © 2023. Indographics. All rights reserved.

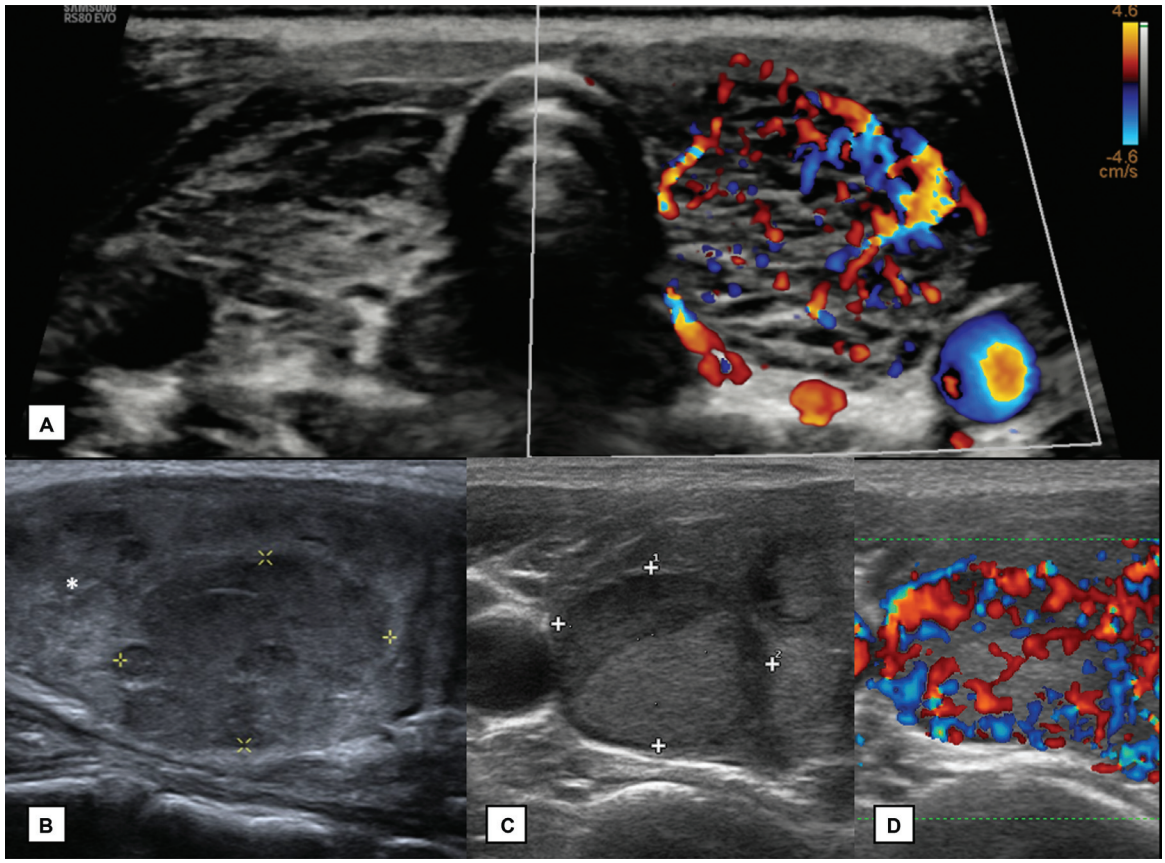

Fig. 7 Thyroiditis. Transverse ultrasound view showing diffusely heterogeneous echotexture of the thyroid with rich internal vascularity (**A**). Solid hypoechoic nodule (TR 4) in a background of thyroiditis seen as diffuse heterogeneous parenchymal echotexture (*asterisk* in **B**). Similar nodule with rich internal vascularity in another patient (**C** and **D**). FNAC proved them to be lymphocytic thyroiditis (**B**) and Hashimoto thyroiditis (**C** and **D**).

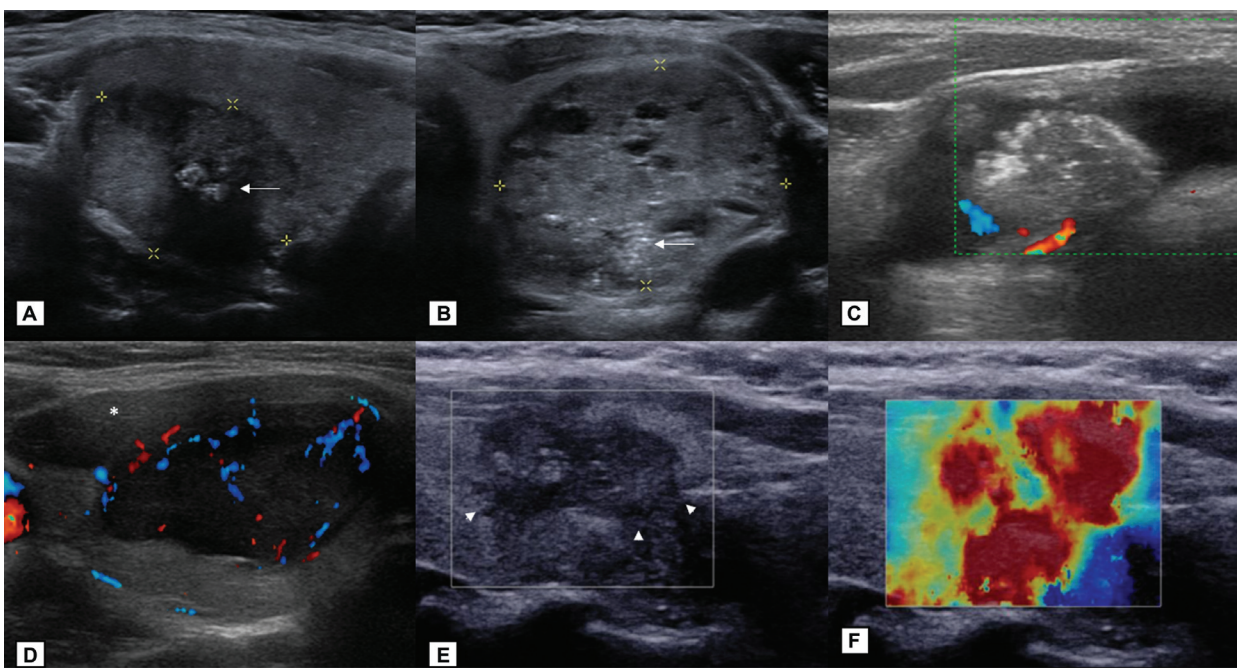

Fig. 8 Papillary carcinoma. Punctate echogenic foci (*arrows*) within hypoechoic (**A**), isoechoic—almost entirely solid (**B**) and solid cystic—isoechoic (**C**) nodules (TR5, TR4, and TR 4, respectively). (**D**) A very hypoechoic nodule as compared with the strap muscle (*asterisk*), with lobulated margins (TR5) and figure (**E**) shows a hypoechoic nodule with irregular margins (*arrowheads*) and punctate echogenic foci (TR5), which is hard on elastography (**F**). All the nodules were diagnosed as papillary carcinomas (Bethesda VI) on FNAC.

 © 2023. Indographics. All rights reserved.

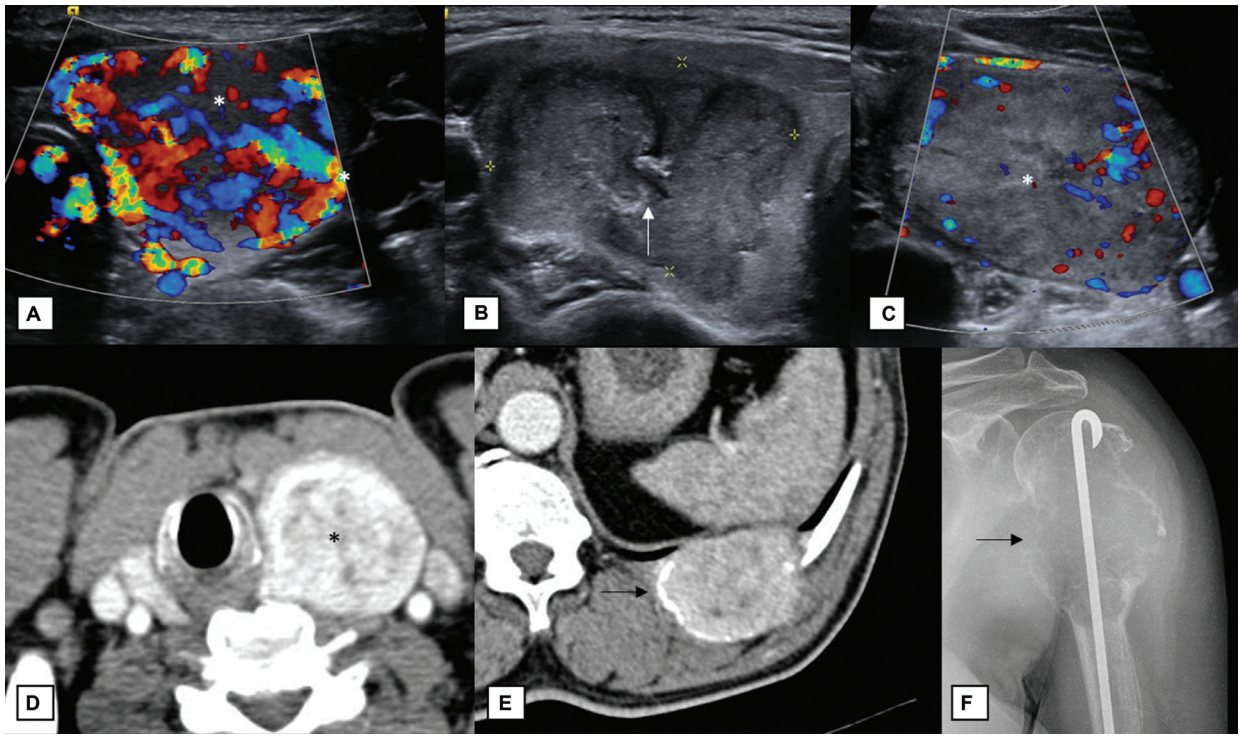

Fig. 9 Follicular neoplasms. A solid hypoechoic nodule (TR 4) with rich vascularity diagnosed to be a follicular neoplasm by FNAC (*asterisk* in **A** [Bethesda IV]). Another solid hypoechoic nodule with microcalcifications (*arrow* in **B**) and lobulated margins (TR 5) diagnosed as follicular variant of papillary carcinoma on FNAC (Bethesda VI), finally proven to be noninvasive follicular thyroid neoplasm with papillary features (NIFTP) on histopathology post thyroidectomy. A TR 4 nodule in left lobe (**C**) on ultrasound, corresponding to a hypoenhancing nodule (*asterisk* in **D**) on CECT, with lytic expansile blow out metastasis of rib and humerus (*arrows* in **E** and **F**), proven to be a follicular carcinoma on histopathological examination.

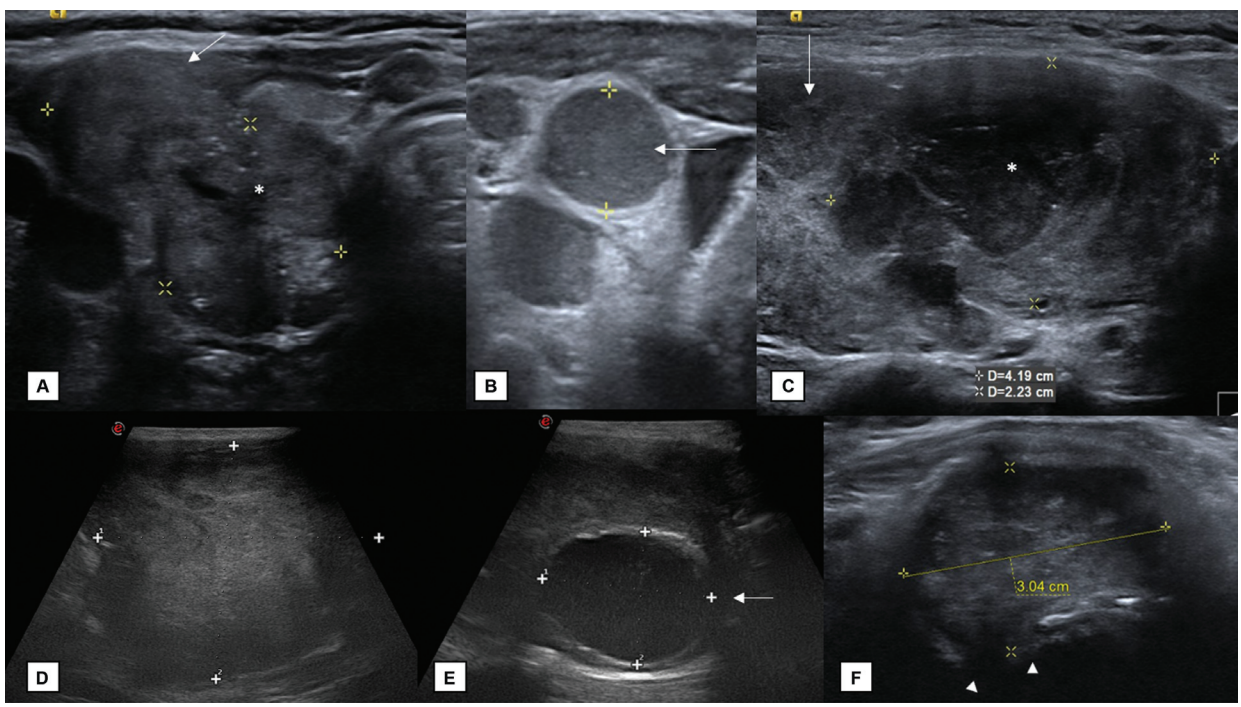

Fig. 10 Medullary carcinoma (**A** and **B**). A solid taller than wide hypoechoic nodule (*asterisk* in **A**) with irregular margins, microcalcifications, and extra thyroid extension (*arrow* in **A**) into strap muscles (TR5), associated round hypoechoic cervical lymph nodes (*arrow* in **B**), proven to be medullary carcinoma on FNAC (Bethesda VI). Lymphoma (**C**). A heterogeneous very hypoechoic nodule (*asterisks*) with lobulated margins (TR 5) with thyroiditis changes in the background parenchyma (*arrow* in c), proven to be diffuse large B cell lymphoma on biopsy. Anaplastic carcinoma (**D–F**). Enlargement of left lobe of thyroid by a large TR 4 nodule (**D**) with internal cystic change and macrocalcification (*arrow* in **E**). Another patient with an ill-defined hypoechoic nodule showing extra thyroid extension into trachea (*arrowheads* in **F**).

 © 2023. Indographics. All rights reserved.

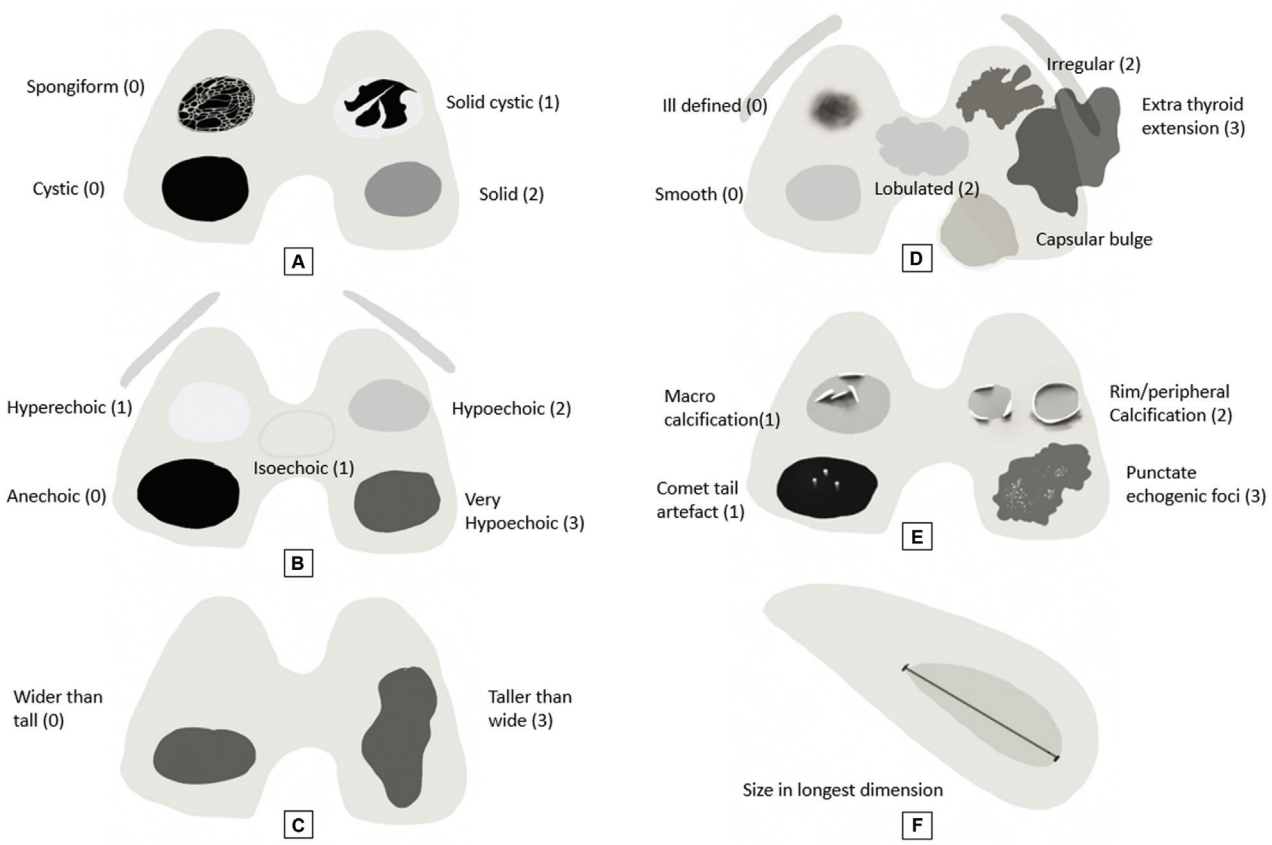

Fig. 11 ACR TI–RADS system. Composition (**A**), echogenicity (**B**), shape (**C**), margin (**D**), and echogenic foci (**E**). The individual scores (within brackets) are added to give a final score and TIRADS category, from which FNAC/follow-up is decided based on the category and size (**F**).

Table 1 Final scoring and FNAC/follow-up guidelines in ACR—TIRADS[24,25]

Points	TR	Risk category	FNAC indication	Follow-up indication	Follow-up time points
0	1	Benign	No	No	–
2	2	Not suspicious	No	No	–
3	3	Mildly suspicious	>2.5 cm	>1.5 cm	1, 3, 5 yr[a]
4–6	4	Moderately suspicious	>1.5 cm	>1 cm	1, 2, 3, 5 yr[a]
≥7	5	Highly suspicious	>1 cm	>0.5 cm	Annually till 5 yr[a]

Abbreviation: FNAC, fine-needle aspiration cytology.
[a]No further follow up after 5 years if there is no increase in size.

than 50% of the nodule, have a high negative predictive value for malignancy.[27]

Echogenicity: Nodules are iso, hypo, or hyperechoic if they are equal to, less than, and more than the echogenicity of the normal thyroid. Nodules are very hypoechoic if they are less echogenic than the strap muscles.[28]

Margins: They can be smooth, ill-defined (more than 50% contour is not made out), lobulated, irregular, or can show overt extrathyroid extension (►**Fig. 10A**) into strap muscles, trachea, esophagus, or larynx, which has the maximum risk of malignancy. The presence of only capsular bulge, border abutment, or loss of echogenic border is considered as minimal extrathyroid extension, the clinical significance of which is controversial.[24]

Shape: Taller than wide orientation (AP dimension greater than T) happens due to the nonuniform growth of malignant cells in different directions. When this feature is combined with solid composition, there is 93% specificity for malignancy.[29]

Calcifications: Dystrophic macrocalcifications with posterior shadowing are commonly seen with benign multinodular goiters. Punctate echogenic foci, which do not show posterior shadowing, correspond to Psammoma bodies histologically and are more commonly seen in malignant nodules.[30] Comet tail artifacts (►**Fig. 5C**) are echogenic foci with additional posterior reverberation in a triangular pattern, which are strongly associated with colloid nodules.

Vascularity: Neoplasms, hyperplasia of follicles, and granulation tissue in colloid nodules can show vascularity.

 © 2023. Indographics. All rights reserved.

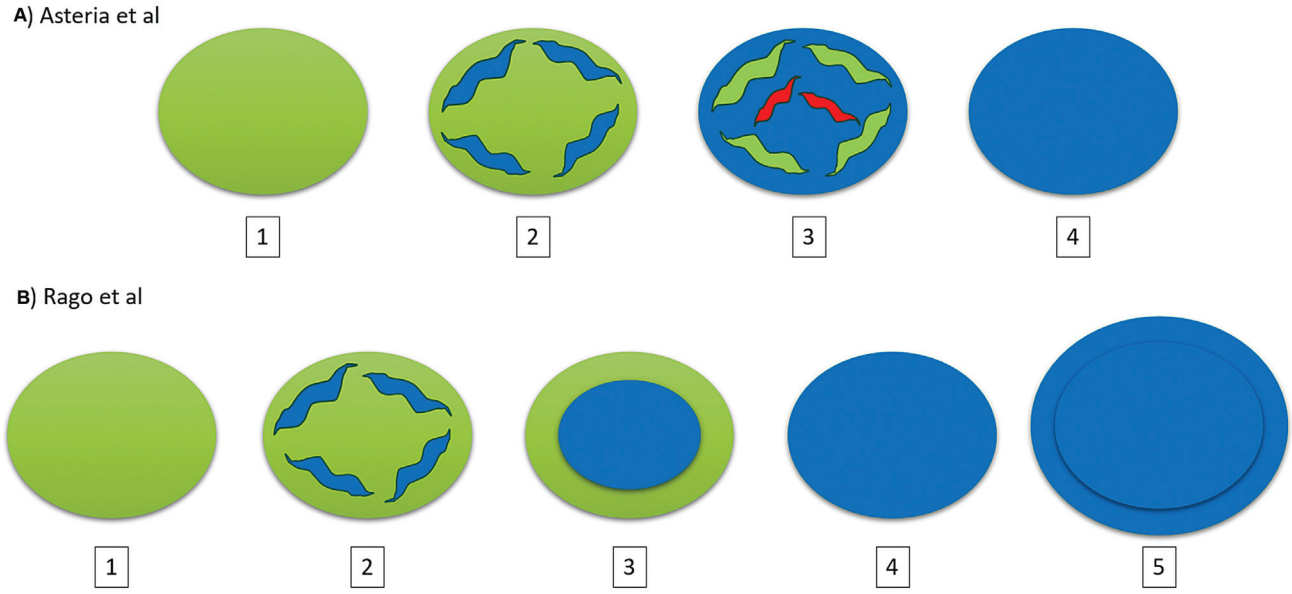

Fig. 12 Schematic representation of the commonly used qualitative SE scores. (**A**) Asteria et al[33] classification—scores: 1 = even elasticity (*green*) in the entire nodule, 2 = elasticity in most part of the nodule, 3 = stiffness (*blue*) in most part, 4 = no elasticity); (**B**) Rago and Vitti et al classification—scores: 1 = Even elasticity (*green*) in the entire nodule, 2 = elasticity in most part of the nodule, 3 = elasticity only in the periphery, 4 = no elasticity, 5 = no elasticity in nodule and the surrounding posterior shadowing).

However, few papillary carcinomas with dense fibrosis may show poor internal vascularity. Power Doppler, more useful than color Doppler, is angle independent, reduces the artifacts and can also help in an accurate depiction of vascularity from small vessels.[31]

Elastography

Strain elastography (SE) by compression: In SE, the stiffness of the tissue is displayed as a color spectrum from red (soft), green (medium), to blue (hard). Qualitative scores (►**Fig. 12**) have been described by Asteria et al (4 points, score 3, or more favoring malignancy) and Rago and Vitti (5 points, score 4, or more favoring malignancy), in the order of increasing stiffness of the nodules.[8,32,33] Semiquantitative evaluation can also be done using strain ratio, comparing the stiffness between the thyroid nodule and surrounding normal parenchyma or muscle. A strain ratio of greater than 1.21 has been found to be the best cut-off in differentiating benign and malignant nodules.[34]

SE by Acoustic radiation force: Qualitative ARFI imaging (►**Figs. 13D** and **13F**) displays tissue stiffness in the form of a grayscale, darker the nodule, more the stiffness. They have been classified into six grades (grade 4 or more favoring malignancy) based on the increasing proportion of darker/blacker areas by Xu et al.[8,35] It was also observed that malignant nodules, owing to their infiltrative margins, show larger areas on elastography images than conventional ultrasound. Nodules were more frequently malignant when the area ratio (area on elastography to that in conventional ultrasound) was greater than 1.09.[36]

Point SWE: In point SWE, the stiffness of tissues is depicted in m/s of the shear wave speed inside a region of interest (ROI) of fixed size (►**Figs. 13E** and **13G**). The median shear wave velocity of normal thyroid parenchyma ranges between 1.2 and 3.6 m/s.[37] The cut-off between benign and malignant nodules with the best diagnostic efficacy ranges between 2.48 and 2.55 m/s.[38] Diffuse thyroid diseases like Hashimoto or Grave's disease may also show high shear wave values of 2.68 ± 0.5 m/s.[8] However, the range of elasticity values that can be depicted is narrow in m/s (usually 0.5–8.4 m/s or 0–10 m/s, depending on the manufacturer) and hence, very hard or very soft tissues are expressed as nonmeasurable ("X.XX m/s").

Two-dimensional SWE: This is available in single shot or real time modes (►**Figs. 6B, –8F, and 13C**) by different vendors. It provides tissue stiffness information in a larger area of user selected box and allows quantitative assessment from multiple ROIs drawn within it. Values are expressed either in m/s (shear wave velocity) or kPa (elasticity), and the color scale is graded from blue (soft) to red (hard).[8] The elasticity values for normal thyroid parenchyma ranges between 10 and 40 kPa. An elasticity value of 65 and 66 kPa in the nodule or an elasticity ratio between the nodule and surrounding normal thyroid of more than 3.7 is considered as the cut-off for malignancy.[37] The values are higher in papillary carcinomas due to their calcifications and fibrous component compared with follicular carcinoma which has more cellular components.[38]

A few pitfalls of elastography include lower stiffness in malignancies with necrosis, cystic areas, and smaller sizes, higher stiffness in benign nodules with calcifications or thyroiditis with more fibrous components, dependence on the application of adequate probe compression, need for including adjacent normal thyroid parenchyma in the field for strain or elasticity ratios which may not be possible in large nodules and varying cut-off values of elastography

 © 2023. Indographics. All rights reserved.

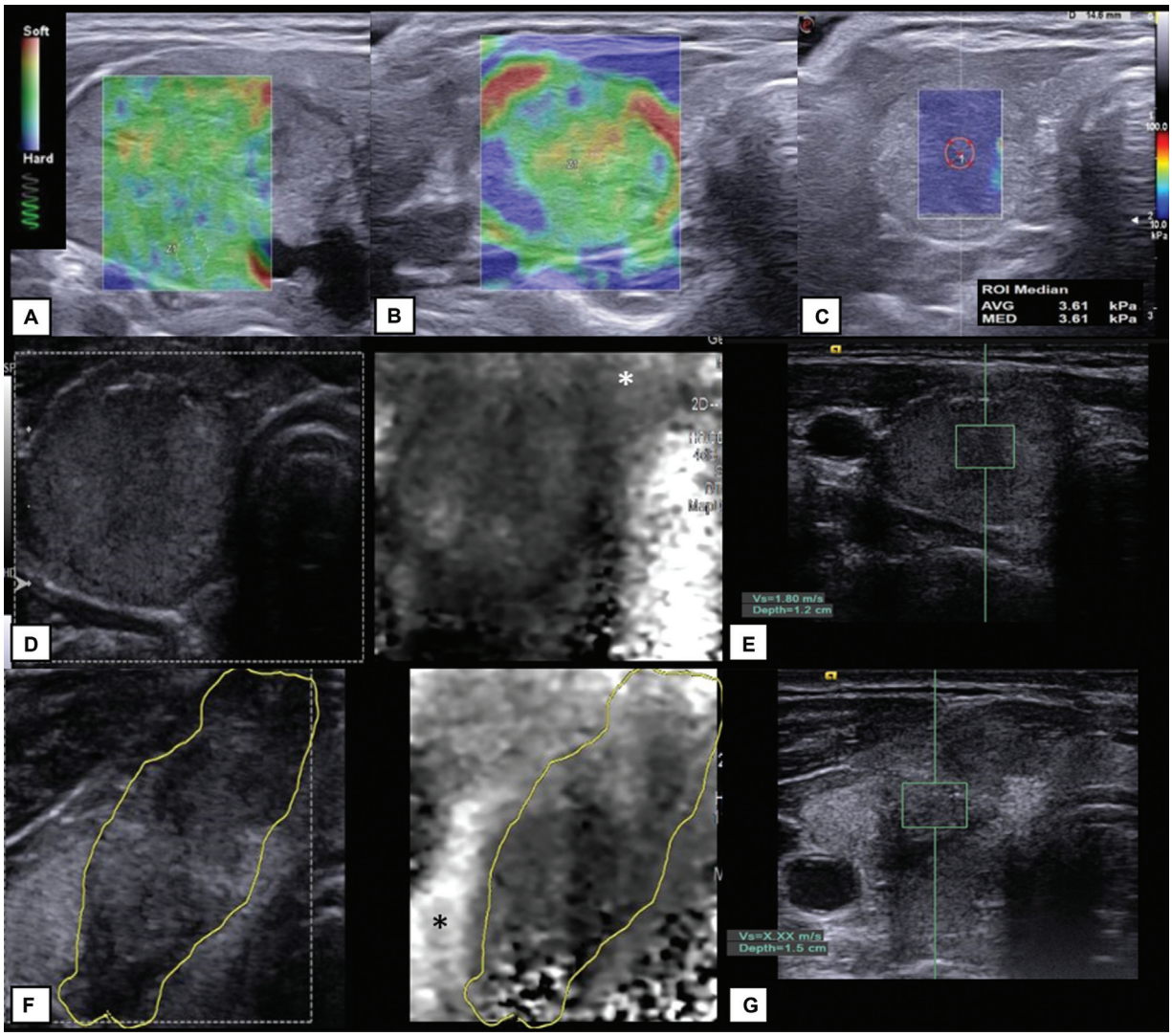

Fig. 13 Elastography of thyroid nodules. Benign nodular goiters showing a qualitative strain elastography score of 2 (**A** and **B**), appearing soft on SWE with elasticity of 3.61 kPa (**C**). Another benign nodular goiter evaluated by qualitative virtual touch imaging (VTi, Siemens), appearing similar to the background parenchyma (*asterisk*) on gray scale, with mean shear wave velocity of 1.8 m/s on point SWE (**D** and **E**). Biopsy-proven medullary thyroid carcinoma, appearing blacker than the background thyroid parenchyma (*asterisk*) on VTi (**F**), with an area of involvement larger than that in the gray scale image, and mean shear wave velocity values X.XX suggesting that it is higher than the highest possible value of 8.4 m/s (**G**).

parameters by different studies to distinguish benign and malignant nodules.

Contrast-Enhanced Ultrasonography

Benign nodules: The patterns of enhancement described in benign nodules (►**Figs. 14** and **15**) include (1) uniform homogeneous or scattered enhancement; (2) iso or hyper-enhancement compared with surrounding normal parenchyma; (3) fast wash-in and slow wash-out; (4) complete hyper- or hypo-enhancing peripheral ring; and (5) no enhancement in cysts.[39–41] The first three features are related to the homogeneous architecture of benign nodules with a relative lack of necrosis or calcifications as well as preserved vascularity within them. Follicular adenomas can show hyperenhancement due to their rich vascularity. A hyper or hypoenhancing rim can be seen due to compression of surrounding thyroid parenchyma and interstitial edema, inflammatory exudates, or the presence of cystic areas within the nodule decompressing the pressure on adjacent parenchyma. Benign nodules with necrosis or a higher proportion of cystic areas, however, may show heterogeneous enhancement.[39–41]

Malignant nodules: In malignancy, necrosis and tumor embolus formation happens within vessels when the growth of the tumor tissue exceeds the vascular supply, which causes hypoenhancement. They also have a heterogeneous composition with varying areas of fibrosis, necrosis, and calcifications within. The enhancement patterns described in CEUS in malignant nodules include (►**Figs. 14** & **15**): (1) hypo-enhancement with nodule to peri-nodule peak intensity ratio less than 0.9,[9,39] (2) heterogeneous enhancement, (3) centripetal enhancement attributed to predominant fibrosis in the central parts, (4) slow wash-in, rapid wash-out ratios and time to peak intensities, although follicular

 © 2023. Indographics. All rights reserved.

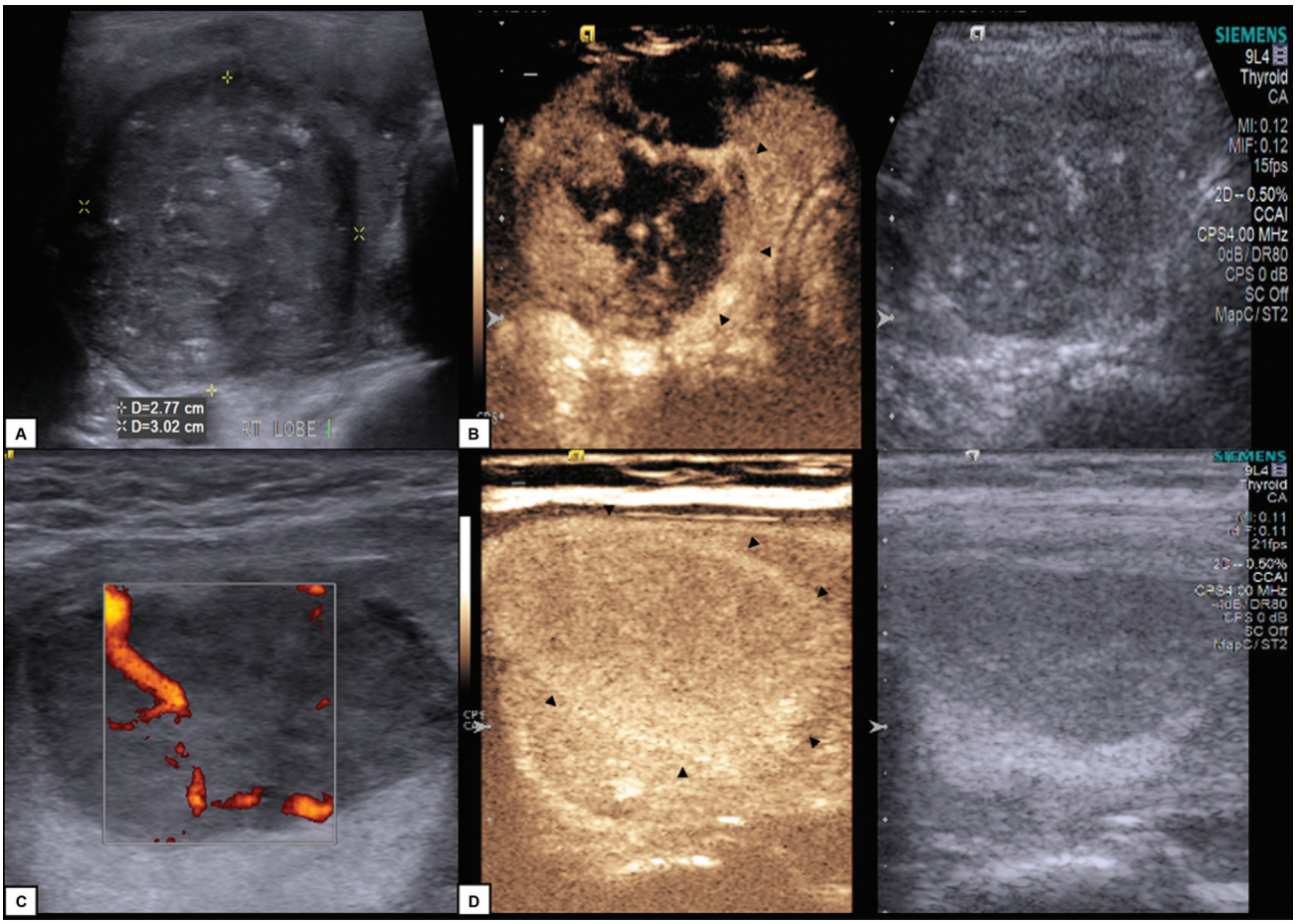

Fig. 14 CEUS enhancement patterns in thyroid nodules. (**A** and **B**) Biopsy-proven papillary carcinoma thyroid seen as a solid hypoechoic nodule with microcalcifications (TR5), with heterogeneous centripetal hypoenhancement pattern on CEUS. An incomplete irregular hyperenhancing ring is seen along part of the nodule (*arrowheads* in **B**). (**C** and **D**) Solid hypoechoic nodule (TR 4) with intranodular vascularity (**C**), showing homogeneous iso enhancement and a complete regular hyperenhacing ring (*arrowheads* in **D**). It was proven to be a nodular goiter by FNAC.

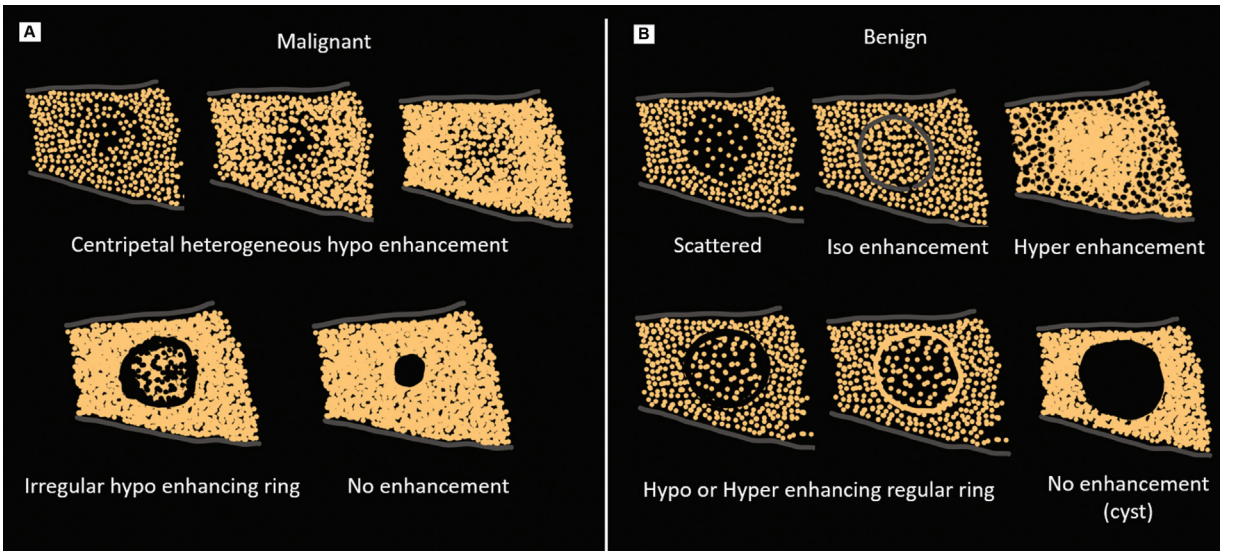

Fig. 15 Schematic diagram of common CEUS enhancement patterns in thyroid nodules. Malignant nodules (**A**) show heterogeneous centripetal hypoenhancement, irregular hypo- or hyper ring enhancement, and sometimes no enhancement in smaller nodules. Benign nodules (**B**) show scattered or equal homogeneous enhancement in all areas, which is equal or more than the background parenchyma, hyper- or hypoenhancing complete regular ring, and no enhancement in cysts.

 © 2023. Indographics. All rights reserved.

carcinomas with rich vascularity show faster wash-in and slow wash-out times just like follicular adenomas, (5) ill-defined enhancement borders, (6) irregular or incomplete ring enhancement (usually hypo- or sometimes hyperenhancing due to peritumoral immune response), (7) no enhancement, particularly in nodules less than 1 cm, and (8) enhancement area smaller or larger than grayscale image.[39–41]

Besides aiding in the differentiation of benign and malignant nodules, they can also help in the follow-up of patients postablation or postradioactive iodine therapy by identifying enhancing viable tissue.[39,42]

Associated Cervical Lymph Nodes

Features of malignant lymph nodal metastasis (►**Figs. 16** and **17**) from the thyroid include[43] hyperechogenicity, round

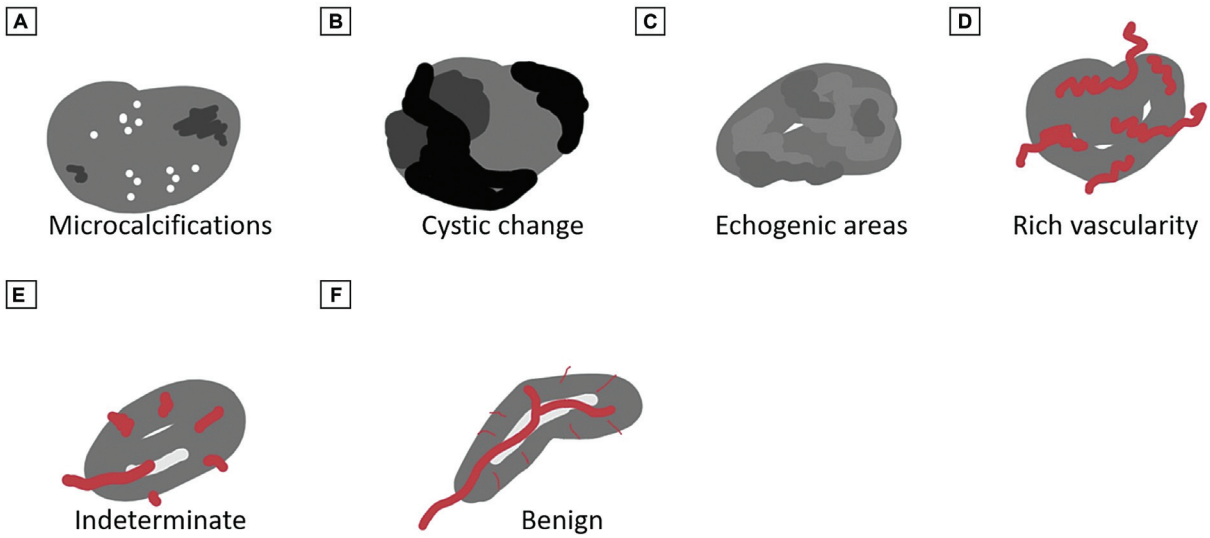

Fig. 16 Schematic diagram of lymph node evaluation in suspected thyroid malignancy. Suspicious features (**A–D**), intermediate suspicion (**E**) when there is loss of echogenic hilum and hilar vascularity, and benign (**F**) when there is the presence of echogenic hilum and hilar vascularity.

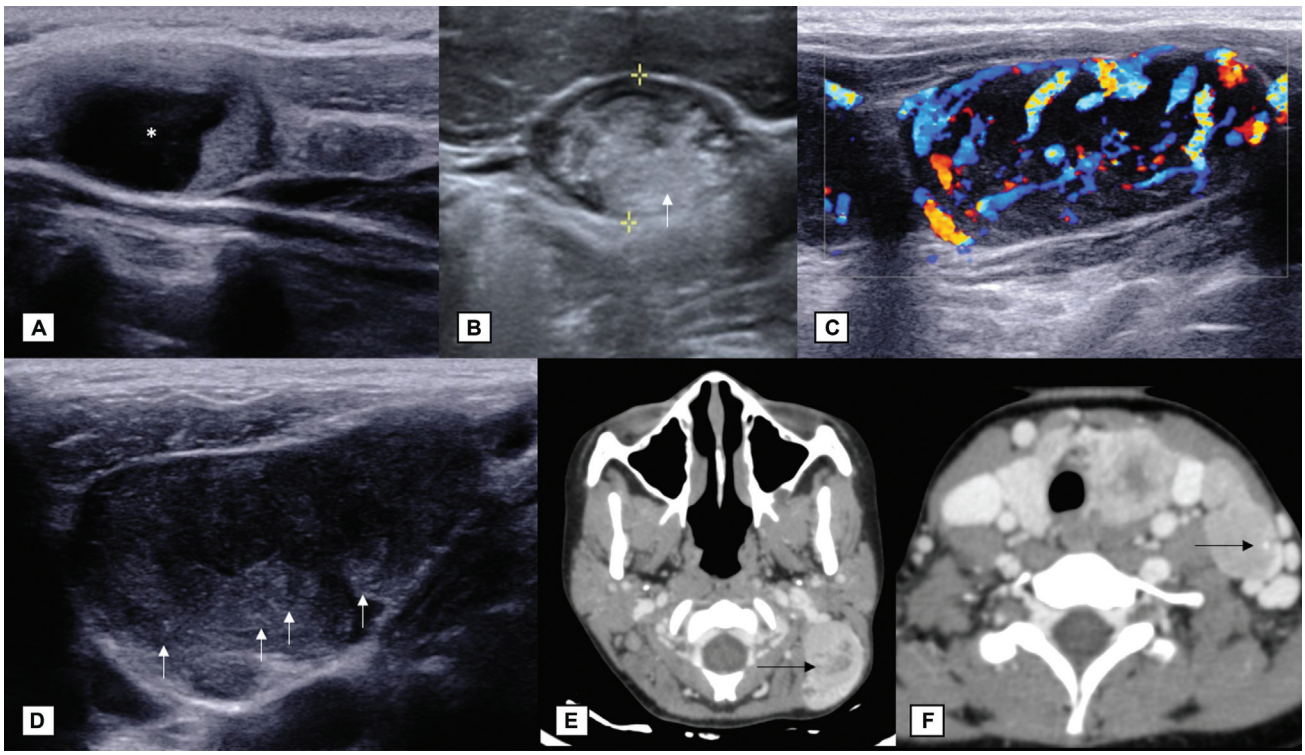

Fig. 17 Lymph node metastasis from papillary carcinoma. Longitudinal views of ultrasound show cystic change (*asterisk* in **A**), hyperechogenicity (*arrow* in **B**), rich vascularity with lost fatty hilum (**C**), and microcalcifications (*arrows* in **D**). Contrast-enhanced CT images show cystic changes within a large left level V lymph node (*arrow* in **E**). Another patient showing calcification within a metastatic node (*arrow* in **F**).

 © 2023. Indographics. All rights reserved.

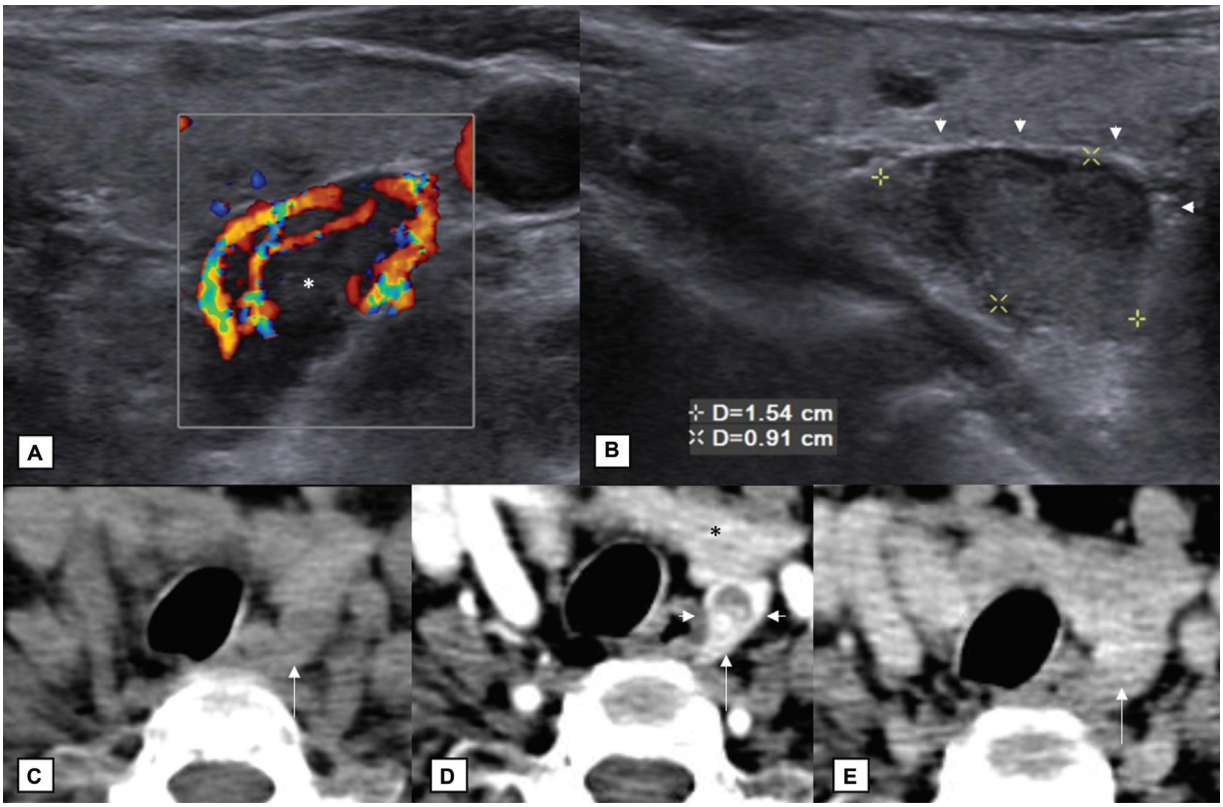

Fig. 18 Parathyroid adenoma. Ultrasound shows a circumscribed hypoechoic lesion (*asterisk*) with rich peripheral vascularity (**A**), separated from the thyroid parenchyma by an echogenic capsule (*arrowheads* in **B**). On contrast-enhanced 4D CT, the lesion (*arrow and arrow heads*) is hypodense on unenhanced section (**C**), intensely enhancing with cystic change and well delineated in the arterial phase (**D**), showing washout in the delayed phase (**E**).

shape, microcalcifications, and cystic change. The presence of cystic areas on ultrasonography is more specific for papillary carcinoma of the thyroid. Echogenic foci can be seen in lymph nodes in both medullary carcinoma (due to amyloid) and papillary carcinoma (due to Psammoma bodies).[44] Metastatic lymph nodes are harder with higher elasticity scores on SWE.[45] On CEUS, malignant lymph nodes show poor vascularization/enhancement areas and perfusion deficits due to necrosis, with centripetal enhancement, while benign nodes show iso and centrifugal enhancement.[42]

Thyroid Nodule Mimic

Parathyroid adenomas commonly occur along the inferior poles of the thyroid, separated from it by an echogenic capsule, and appear as hypoechoic solid lesions with feeding polar vessels[46] (►**Fig. 18**). In approximately 1 to 7% cases, they can be completely or partially intrathyroid and can be confused with a thyroid nodule.[47] Four-dimensional computerized tomography can help to differentiate between thyroid nodules and parathyroid lesions, as the latter show arterial hyperenhancement, washout, and polar vessels.[48]

Conclusion

To summarize, thyroid pathologies include a wide spectrum of diseases involving adults as well as children. Ultrasound is the imaging modality of choice, which can serve as a screening, diagnostic, and sometimes a problem-solving tool. Knowledge of the embryological anatomy can help in differentiating complex congenital thyroid pathologies from other neck pathologies. Meticulous application of TIRADS can help to set apart suspicious nodules which require FNAC and those which can be followed up.

Author Contributions
S.L.M. was responsible for design, literature search, manuscript preparation; R.G. was responsible for manuscript editing, manuscript review; S.V.C. was responsible for manuscript review; M.R. was responsible for manuscript preparation; and K.V. was responsible for manuscript preparation.

Funding
None.

Conflict of Interest
None declared.

Acknowledgments
The authors wish to extend their gratitude to Dr. Sabarish S for contributing elastography images.

References

1 Unnikrishnan AG, Menon UV. Thyroid disorders in India: an epidemiological perspective. Indian J Endocrinol Metab 2011; 15(Suppl 2):S78–S81

 © 2023. Indographics. All rights reserved.

2 Popoveniuc G, Jonklaas J. Thyroid nodules. Med Clin North Am 2012;96(02):329–349
3 Welker MJ, Orlov D. Thyroid nodules. Am Fam Physician 2003;67 (03):559–566
4 Stathatos N. Anatomy and physiology of the thyroid gland. In: The Thyroid and Its Diseases. Springer. 2019:3–12
5 Policeni BA, Smoker WRK, Reede DL. Anatomy and embryology of the thyroid and parathyroid glands. Semin Ultrasound CT MR 2012;33(02):104–114
6 Gallo M, Pesenti M, Valcavi R. Ultrasound thyroid nodule measurements: the "gold standard" and its limitations in clinical decision making. Endocr Pract 2003;9(03):194–199
7 Loevner LA. Imaging of the thyroid gland. Semin Ultrasound CT MR 1996;17(06):539–562
8 Zhao CK, Xu HX. Ultrasound elastography of the thyroid: principles and current status. Ultrasonography 2019;38(02):106–124
9 Zhan J, Ding H. Application of contrast-enhanced ultrasound for evaluation of thyroid nodules. Ultrasonography 2018;37(04): 288–297
10 Taş F, Bulut S, Eğilmez H, Oztoprak I, Ergür AT, Candan F. Normal thyroid volume by ultrasonography in healthy children. Ann Trop Paediatr 2002;22(04):375–379
11 Hong HS, Lee EH, Jeong SH, Park J, Lee H. Ultrasonography of various thyroid diseases in children and adolescents: a pictorial essay. Korean J Radiol 2015;16(02):419–429
12 Marinovic D, Garel C, Czernichow P, Léger J. Additional phenotypic abnormalities with presence of cysts within the empty thyroid area in patients with congenital hypothyroidism with thyroid dysgenesis. J Clin Endocrinol Metab 2003;88(03):1212–1216
13 Zander DA, Smoker WRK. Imaging of ectopic thyroid tissue and thyroglossal duct cysts. Radiographics 2014;34(01):37–50
14 Rabinov K, Van Orman P, Gray E. Radiologic findings in persistent thyroglossal tract fistulas. Radiology 1979;130(01):135–139
15 Nachiappan AC, Metwalli ZA, Hailey BS, Patel RA, Ostrowski ML, Wynne DM. The thyroid: review of imaging features and biopsy techniques with radiologic-pathologic correlation. Radiographics 2014;34(02):276–293
16 Anderson L, Middleton WD, Teefey SA, et al. Hashimoto thyroiditis: Part 1, sonographic analysis of the nodular form of Hashimoto thyroiditis. AJR Am J Roentgenol 2010;195(01):208–215
17 Langer JE, Khan A, Nisenbaum HL, et al. Sonographic appearance of focal thyroiditis. AJR Am J Roentgenol 2001;176(03):751–754
18 Pishdad P, Pishdad GR, Tavanaa S, Pishdad R, Jalli R. Thyroid ultrasonography in differentiation between Graves' disease and Hashimoto's thyroiditis. J Biomed Phys Eng 2017;7(01):21–26
19 Kuo TC, Wu MH, Chen KY, Hsieh MS, Chen A, Chen CN. Ultrasonographic features for differentiating follicular thyroid carcinoma and follicular adenoma. Asian J Surg 2020;43(01):339–346
20 Kim DS, Kim JH, Na DG, et al. Sonographic features of follicular variant papillary thyroid carcinomas in comparison with conventional papillary thyroid carcinomas. J Ultrasound Med 2009;28 (12):1685–1692
21 Liu MJ, Liu ZF, Hou YY, et al. Ultrasonographic characteristics of medullary thyroid carcinoma: a comparison with papillary thyroid carcinoma. Oncotarget 2017;8:27520–27528
22 Xia Y, Wang L, Jiang Y, Dai Q, Li X, Li W. Sonographic appearance of primary thyroid lymphoma-preliminary experience. PLoS One 2014;9(12):e114080
23 Nixon IJ, Coca-Pelaz A, Kaleva AI, et al. Metastasis to the thyroid gland: a critical review. Ann Surg Oncol 2017;24(06):1533–1539
24 Tessler FN, Middleton WD, Grant EG, et al. ACR Thyroid Imaging, Reporting and Data System (TI-RADS): White Paper of the ACR TI-RADS Committee. J Am Coll Radiol 2017;14(05):587–595
25 Tappouni RR, Itri JN, McQueen TS, Lalwani N, Ou JJ. ACR TI-RADS: pitfalls, solutions, and future directions. Radiographics 2019;39 (07):2040–2052
26 Frates MC, Benson CB, Charboneau JW, et al; Society of Radiologists in Ultrasound. Management of thyroid nodules detected at US: Society of Radiologists in Ultrasound consensus conference statement. Radiology 2005;237(03):794–800
27 Moon WJ, Jung SL, Lee JH, et al; Thyroid Study Group, Korean Society of Neuro- and Head and Neck Radiology. Benign and malignant thyroid nodules: US differentiation–multicenter retrospective study. Radiology 2008;247(03):762–770
28 Hoang JK, Lee WK, Lee M, Johnson D, Farrell S. US Features of thyroid malignancy: pearls and pitfalls. Radiographics 2007;27 (03):847–860, discussion 861–865
29 Kim EK, Park CS, Chung WY, et al. New sonographic criteria for recommending fine-needle aspiration biopsy of nonpalpable solid nodules of the thyroid. AJR Am J Roentgenol 2002;178 (03):687–691
30 Taki S, Terahata S, Yamashita R, et al. Thyroid calcifications: sonographic patterns and incidence of cancer. Clin Imaging 2004;28(05):368–371
31 Moon HJ, Kwak JY, Kim MJ, Son EJ, Kim EK. Can vascularity at power Doppler US help predict thyroid malignancy? Radiology 2010;255(01):260–269
32 Rago T, Vitti P. Role of thyroid ultrasound in the diagnostic evaluation of thyroid nodules. Best Pract Res Clin Endocrinol Metab 2008;22(06):913–928
33 Asteria C, Giovanardi A, Pizzocaro A, et al. US-elastography in the differential diagnosis of benign and malignant thyroid nodules. Thyroid 2008;18(05):523–531
34 Chong Y, Shin JH, Ko ES, Han BK. Ultrasonographic elastography of thyroid nodules: is adding strain ratio to colour mapping better? Clin Radiol 2013;68(12):1241–1246
35 Xu JM, Xu XH, Xu HX, et al. Conventional US, US elasticity imaging, and acoustic radiation force impulse imaging for prediction of malignancy in thyroid nodules. Radiology 2014;272 (02):577–586
36 Xu JM, Xu HX, Zhang YF, et al. Virtual touch tissue imaging for differential diagnosis of thyroid nodules: additional value of the area ratio. J Ultrasound Med 2016;35(05):917–926
37 Monpeyssen H, Tramalloni J, Poirée S, Hélénon O, Correas JM. Elastography of the thyroid. Diagn Interv Imaging 2013;94(05): 535–544
38 Li J, Zhang YR, Ren JY, et al. Association between diagnostic efficacy of acoustic radiation force impulse for benign and malignant thyroid nodules and the presence or absence of non-papillary thyroid cancer: a meta-analysis. Front Oncol 2023; 13:1007464
39 Radzina M, Ratniece M, Putrins DS, Saule L, Cantisani V. Performance of contrast-enhanced ultrasound in thyroid nodules: review of current state and future perspectives. Cancers (Basel) 2021;13(21):5469
40 Ruan J, Xu X, Cai Y, et al. A practical CEUS thyroid reporting system for thyroid nodules. Radiology 2022;305(01):149–159
41 Zhang Y, Zhang MB, Luo YK, Li J, Wang ZL, Tang J. The value of peripheral enhancement pattern for diagnosing thyroid cancer using contrast-enhanced ultrasound. Int J Endocrinol 2018;2018: e1625958
42 Sorrenti S, Dolcetti V, Fresilli D, et al. The role of CEUS in the evaluation of thyroid cancer: from diagnosis to local staging. J Clin Med 2021;10(19):4559
43 Ha EJ, Chung SR, Na DG, et al. 2021 Korean thyroid imaging reporting and data system and imaging-based management of thyroid nodules: Korean Society of Thyroid Radiology Consensus Statement and Recommendations. Korean J Radiol 2021;22(12): 2094–2123
44 Ahuja AT, Chow L, Chick W, King W, Metreweli C. Metastatic cervical nodes in papillary carcinoma of the thyroid: ultrasound and histological correlation. Clin Radiol 1995;50(04):229–231

 © 2023. Indographics. All rights reserved.

45 Jung WS, Kim JA, Son EJ, Youk JH, Park CS. Shear wave elastography in evaluation of cervical lymph node metastasis of papillary thyroid carcinoma: elasticity index as a prognostic implication. Ann Surg Oncol 2015;22(01):111–116
46 Sung JY. Parathyroid ultrasonography: the evolving role of the radiologist. Ultrasonography 2015;34(04):268–274
47 Goodman A, Politz D, Lopez J, Norman J. Intrathyroid parathyroid adenoma: incidence and location—the case against thyroid lobectomy. Otolaryngol Head Neck Surg 2011;144(06):867–871
48 Hoang JK, Sung WK, Bahl M, Phillips CD. How to perform parathyroid 4D CT: tips and traps for technique and interpretation. Radiology 2014;270(01):15–24

 © 2023. Indographics. All rights reserved.